coatings

MDPI

Article

Tire/Road Rolling Resistance Modeling: Discussing the Surface Macrotexture Effect

Malal Kane *, Ebrahim Riahi and Minh-Tan Do

AME-EASE, University Gustave Eiffel, IFSTTAR, F-44344 Bouguenais, France; Ebrahim.riahi@univ-eiffel.fr (E.R.); minh-tan.do@univ-eiffel.fr (M.-T.D.)

* Correspondence: malal.kane@univ-eiffel.fr

Abstract: This paper deals with the modeling of rolling resistance and the analysis of the effect of pavement texture. The Rolling Resistance Model (RRM) is a simplification of the no-slip rate of the Dynamic Friction Model (DFM) based on modeling tire/road contact and is intended to predict the tire/pavement friction at all slip rates. The experimental validation of this approach was performed using a machine simulating tires rolling on road surfaces. The tested pavement surfaces have a wide range of textures from smooth to macro-micro-rough, thus covering all the surfaces likely to be encountered on the roads. A comparison between the experimental rolling resistances and those predicted by the model shows a good correlation, with an R^2 exceeding 0.8. A good correlation between the MPD (mean profile depth) of the surfaces and the rolling resistance is also shown. It is also noticed that a random distribution and pointed shape of the summits may also be an inconvenience concerning rolling resistance, thus leading to the conclusion that beyond the macrotexture, the positivity of the texture should also be taken into account. A possible simplification of the model by neglecting the damping part in the constitutive model of the rubber is also noted.

Keywords: dynamic friction model; rolling resistance coefficient; macrotexture

check for updates

Citation: Kane, M.; Riahi, E.; Do, M.-T. Tire/Road Rolling Resistance Modeling: Discussing the Surface Macrotexture Effect. *Coatings* **2021**, *11*, 538. https://doi.org/10.3390/coatings11050538

Academic Editor: Claudio Lantieri

Received: 13 April 2021
Accepted: 28 April 2021
Published: 2 May 2021

Publisher's Note: MDPI stays neutral with regard to jurisdictional claims in published maps and institutional affiliations.

Copyright: © 2021 by the authors. Licensee MDPI, Basel, Switzerland. This article is an open access article distributed under the terms and conditions of the Creative Commons Attribution (CC BY) license (https://creativecommons.org/licenses/by/4.0/).

1. Introduction

Energy-efficient transportation systems are becoming an increased societal demand, especially in the current context, where ecology is becoming a global issue [1]. Therefore, in the road transport sector, huge efforts have been put into both vehicles [2] and infrastructure to minimize fuel consumption—in particular, through the reduction in the rolling resistance [3]. Indeed, the lower the rolling resistance is, the less energy is required to move vehicles forward; a low rolling resistance can mean 0.25 L less fuel per 100 km driven [4]. This amount may not seem impressive, but because the distance traveled by a European driver is about 20,000 km per year, the savings will be felt.

Regarding another aspect of vehicles and, in particular, the contact of their tires on roads, huge efforts have been made by tire manufacturers to reduce their rolling resistance as much as possible without reducing their efficiency in terms of skid resistance and rolling noise [5]. Regarding another aspect of roads, even if substantial effort is made in the design of road structures to minimize their contribution to rolling resistance, the effect of the surface texture, in particular the macrotexture, on this rolling resistance remains largely unknown [6,7].

For the measurement methods [8–11], beyond the coast-down method, there are more sophisticated ones. An example is a technology developed in the context of the project OPTYRE [12], where a wireless optical system permits the direct observation of the inner tire stress when rolling; following a developed tire model, the authors identified the instant rolling resistance. However, no reference has been made to the possible use of such a system to identify the effect of the road surface texture.

There have already been experimental attempts to evaluate the contribution of macrotexture to rolling resistance. One example is the EU-funded MIRIAM project, as already

highlighted above, where several devices, often trailers towed by a vehicle measuring the torque on the axis of the tire in free-rolling, have carried out cross-trials on the Nantes test track of the Gustave Eiffel University. This test facility has the particular ability to present surfaces with different textures. The test results showed an overall increase in rolling resistance with macrotexture [13].

In terms of rolling resistance modeling [14,15], proposals are often finite element-based approaches. These approaches generally allow predictions of the contribution of the tires or the pavement structure to rolling resistance but are often not fine enough to evaluate the contribution of the macrotexture [16]. Indeed, FEMs are generally not fine enough in terms of mesh size to take into account the surface texture and thus evaluate its contribution [17]. There are also much simpler approaches, such as from Chalmers University, dedicated to the understanding of the physics behind the contribution of tires only [18]. The Chalmers' model, where the rolling resistance coefficient is the ratio of the offset length of the deformed radius of the tire, does not take into account the texture either.

The present paper tries to go further by proposing another exploitation of the Dynamic Friction Model (DFM) (renamed here Rolling Resistance Model (RRM)) to take into account the contribution of the pavement macrotexture in the generation of rolling resistance. The RRM thus derives from the simplification of the DFM by eliminating the sliding in tire/road contact and is used to predict the coefficient of rolling resistance (Crr) on several surfaces with different macrotextures [19,20]. The experimental validation was performed using a device that simulates the rolling of tires on road surfaces [21]. The first section of this paper will present the RRM and the algorithm behind the numerical calculation program. The second section will be dedicated to the experimental part of the RRM validation and will be followed by the last two parts, which will discuss the results.

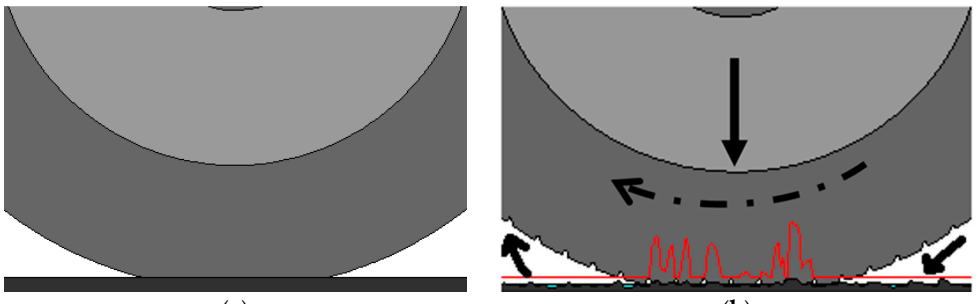
2. Modeling

2.1. From DFM to RRM: Adaptation of the Dynamic Friction Model to the Modeling of Rolling Resistance

An adaptation of the DFM (which predicts the tire/pavement friction from 0 to 1 slip rates) was made by limiting the cinematic movement in the contact to pure rolling of the tire without any slip [19]. The rolling resistance predictions are then based on the calculation of the tangential forces generated in the contact area between the rolling tire and the rough road surface. This force, tending to oppose the forward movement of the tire, is assumed to partially originate from the unsymmetrical envelopment of the surface asperities by the rolling tire tread.

2.2. Two Steps Calculation

The calculation procedure was conducted in two steps: The first step was to determine the apparent contact area. This step was completed in a static mode and by considering the road surface as smooth (Figure 1a). The second step was to coat the deformed tire (first step) with its grooved tread of rubber material and, afterward, roll it upon the rough road surface (Figure 1b).



(**a**) (**b**)

Figure 1. The two calculation steps. The first step determines the apparent contact area assuming the tire static on a smooth road (**a**). The second step determines the real contact area and thus the rolling resistance with the rolling tire upon the rough road surface (**b**).

2.3. Calculating the Rolling Resistance Coefficient (Crr)

The governing equations (Equations (1)–(5)) are derived from the balance of the forces acting in the contact area [19]. The tire tread and the road surface are discretized, and both tire and road elements are identified with a single index i (unlike the DFM, where, due to the possible tire slip, two different indices are used). Thus, i identifies both rubber and tire elements facing each other. Indeed, when the tire rolls on the road surface, each of its elements keeps contact with the same element of the road surface during its entire contact duration.

$$\vec{F_i} + \vec{T_i} + \vec{R_i} + \vec{FR_i} = \vec{0}, \quad (1)$$

where $\vec{F_i}$ is the local contact force applied by the rubber element (due to its deformation) on the surface element. In the present work, a Kelvin–Voigt model is used for the rubber, where K is the spring's stiffness and C is the dashpot's viscosity. $\vec{F_i}$ is balanced by the load through the contact pressure p_i, the width of the tire l, and the distance between two successive points (corresponding to the capture resolution of the surface) dx. $F_i(t) = l \times dx \times p_i(t)$ with $p_i(t) = Ku_i(t) + C\frac{du_i(t)}{dt}$ and $u_i(t) = \delta(t) - h_i + z_i$, with t representing the time. $u_i(t)$ is the displacement of the tread ith element contacting the ith element on the road. $\delta(t)$ is the solid displacement of the tire at t. h_i represents the tire geometry. z_i is the height of the ith point of the road profile.

$\vec{T_i}$ is the traction force. This force must be equal to or just greater than the rolling resistance force opposing the movement.

$\vec{R_i}$ is the local normal surface reaction force.

$\vec{FR_i}$ is the local friction force. $FR_i = \mu_{loc} R_i$ when the element is moving on a "pseudo smooth inclined plan" with angle α_i. μ_{loc} represents a local friction coefficient corresponding to the actual adhesion coefficient and/or a local hysteresis coefficient, accounting for the contribution of the asperities with wavelengths smaller than the captured resolution of the surface texture.

The projection of Equation (1) onto axes x and z leads to:

$$T_i(t) = F_i(t)\frac{\sin(\alpha_i) + \mu_{loc}\cos(\alpha_i)}{\cos(\alpha_i) - \mu_{loc}\sin(\alpha_i)}. \quad (2)$$

When a tread element is not in contact with the road surface, its contact pressure is nil and the element is subjected to a relaxation phase. At any time t, the total normal load W applied by the tire on the road surface must be balanced by the normal contact pressure:

$$W = \sum_i^N F_i(t), \quad (3)$$

where N is the number of elements comprising the tire tread in the contact area. Accordingly, the global rolling resistance coefficient $Crr_i(t)$ can then be calculated using the following formula:

$$Crr_i(t) = \frac{\sum_i^N T_i(t)}{W}. \quad (4)$$

2.4. Calculation Algorithm

At this stage, the only unknown is $F_i(t)$. The calculation was conducted in two steps, as already explained above: the first step was to evaluate the apparent contact area and the second step was to evaluate the actual local contact areas (real contact area), pressure distribution, rolling resistance force, and finally the rolling resistance coefficient. Figure 2 illustrates the algorithm behind the numerical calculation program. The algorithm may be implemented with any programming language. If it is well written, the calculation code gives the Crr at each time step (i.e., at each loop of the dynamic part of the program).

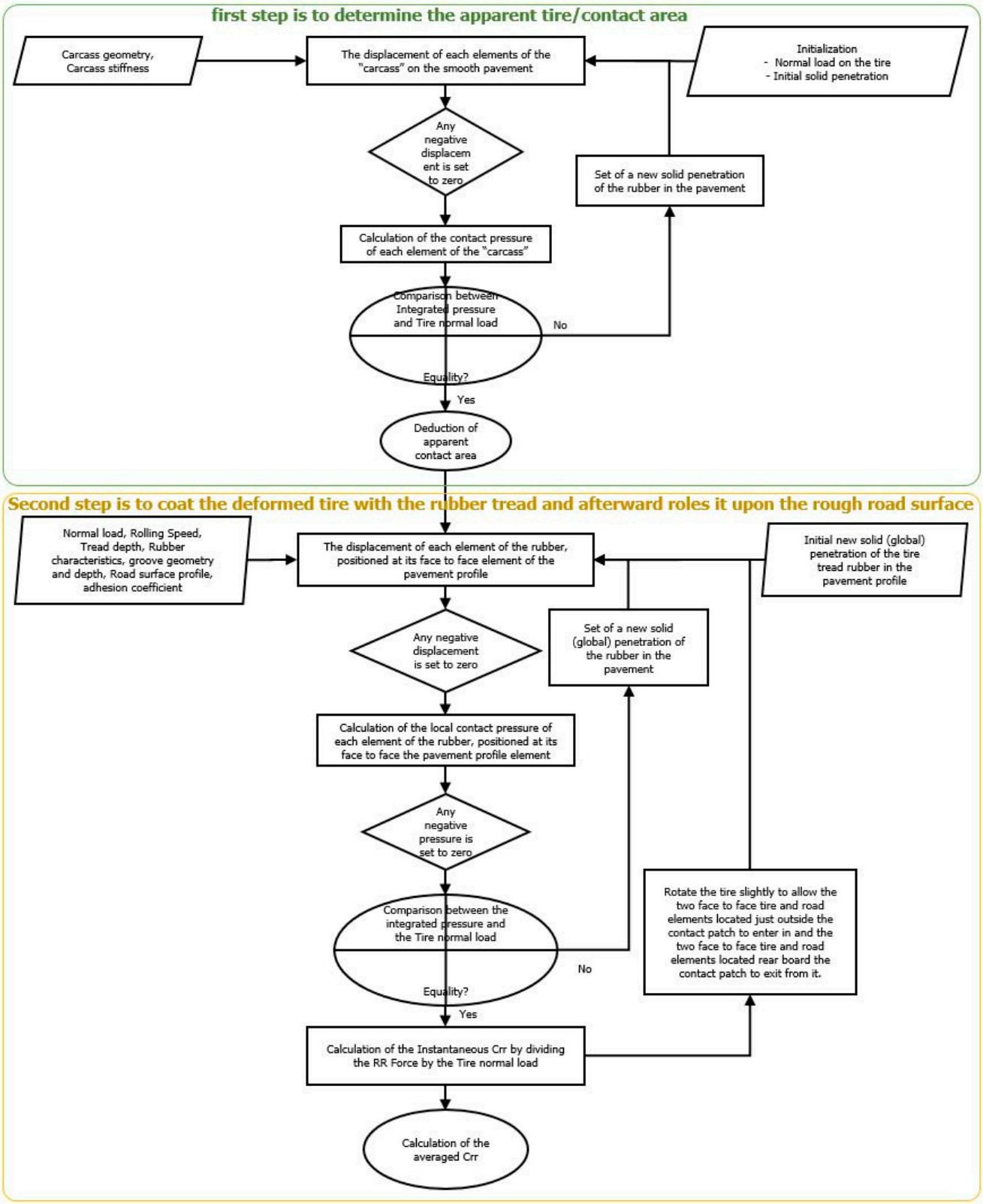


Figure 2. Algorithm of the Crr numerical calculation program.

3. Experiments

3.1. Measuring the Rolling Resistance Coefficient

The Wehner/Schulze machine-polishing unit was used to measure the Crr (Figure 3a) [21]. This unit is composed of a rotary head equipped with three rubber cones with a superior and inferior diameter of 80 and 36 mm, respectively (Figure 3b). These three cones rolled on the road surfaces to be tested with a normal load of 392 N. The road specimen was placed inside a fixed holder (Figure 3c) equipped with a dynamometer sensor to measure the resistant torque due to the cone rolling (Figure 3d).

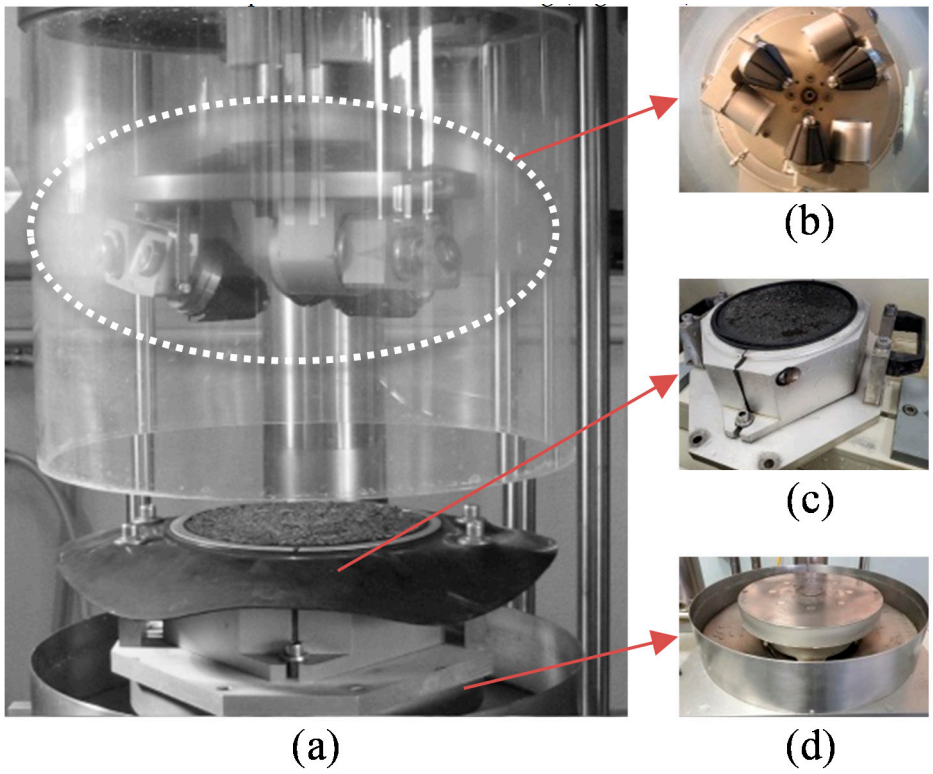


Figure 3. (**a**) Polishing unit; (**b**) rotating head; (**c**) sample holder; (**d**) torque measuring base.

The Crr was then deducted from the measured torque, the normal load, and the radius of the sample holder (Equation (5)).

$$\mathrm{Crr} = \frac{\mathrm{M_r}}{\mathrm{rW}}, \tag{5}$$

where $\mathrm{M_r}$ represents the measured resistant torque, W the applied normal load, and r (82.25 mm) the holder radius (distance between the center of the sample and the center of the cones).

3.2. Tested Surfaces

The seven tested surfaces were disc samples of 225 mm in diameter cored from the Gustave Eiffel University test track located in Nantes and represent a wide range of textures from smooth (Tile) to macro-micro-rough. These surfaces were chosen because of the variety of macrotextures they present. In fact, they range from smooth to different levels of macrotexture that can in turn be positive or negative. Their profiles were also captured with a profilometer to serve as input to the RRM and to calculate their "Mean Profile Depths" (MPD), the index chosen to characterize their macrotexture. Table 1 displays the details of these surfaces, the size of the aggregates used to make them, and the photos of the samples.

Table 1. Test surfaces and their characteristics.

Name	Description	MPD	Surface Texture
Tile	Smooth	0.02	
E1	Semi-coarse asphalt concrete	0.27	
E2	Semi-coarse asphalt concrete	0.53	
A	Porous asphalt concrete	0.34	
M2	Very thin asphalt concrete	0.35	
F	Hight-friction dressing «COLGRIP©»	0.69	
M1	Very thin asphalt concrete	0.69	

Figure 4 shows examples of profiles captured from these surfaces that were used to calculate the MPD and will serve as input to the model to calculate the Crr.

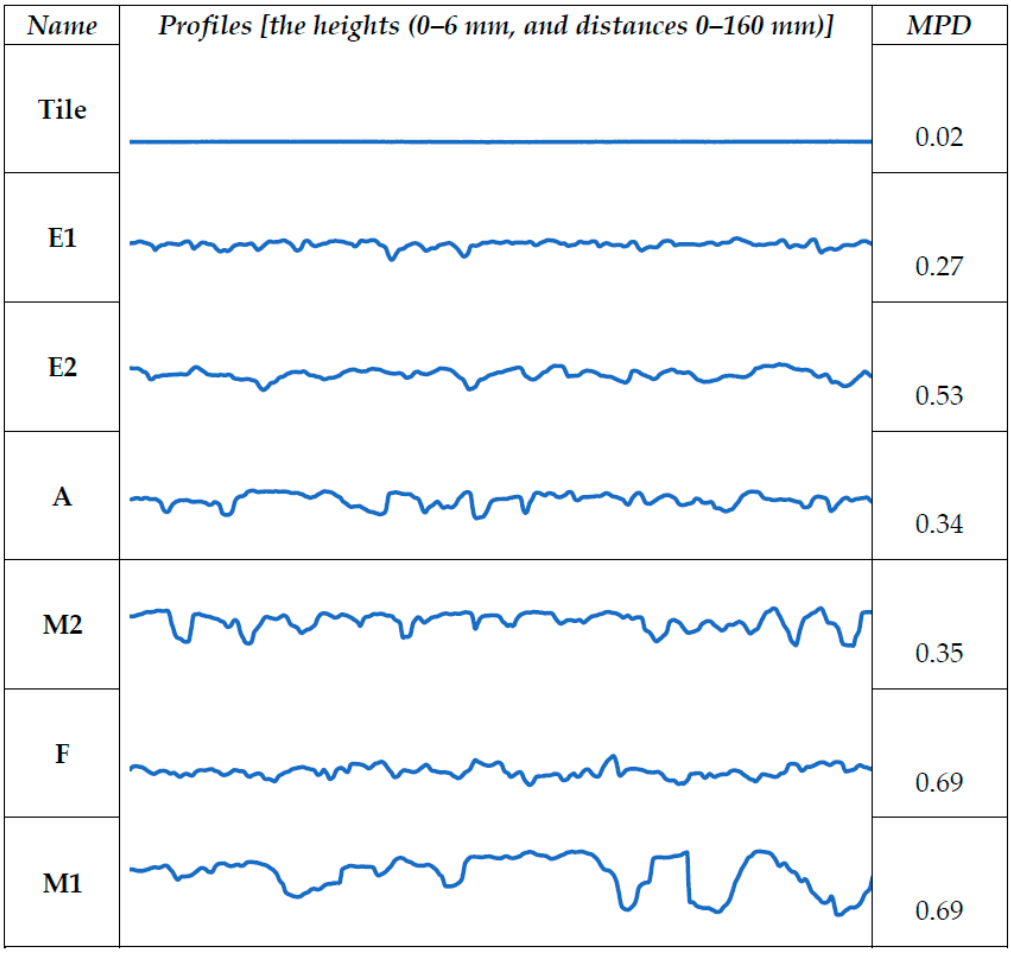


Figure 4. Profiles captured from these surfaces and their estimated MPD.

4. Results

Table 2 shows the Crr results of the RRM predictions (Crr_RRM) and those measured with the WS machine (Crr_WS) on the seven surfaces. The last column of the table shows the MPD calculated from the profiles of these surfaces.

Table 2. Crr_RRM and Crr_WS of each test surface.

Surfaces	MPD	Crr_RRM	Crr_WS
Tile	0.02	1.30×10^{-3}	8.75×10^{-2}
E1	0.27	3.42×10^{-2}	9.34×10^{-2}
E2	0.53	5.19×10^{-2}	9.56×10^{-2}
A	0.34	5.36×10^{-2}	9.24×10^{-2}
M2	0.35	4.65×10^{-2}	9.34×10^{-2}
F	0.69	8.15×10^{-2}	9.97×10^{-2}
M1	0.69	6.27×10^{-2}	1.00×10^{-1}

Figure 5 shows the correlation line between the Crr_RRM and Crr_WS. A good correlation was noticed with an R^2 of 0.8, even though there was a factor close to two between the measured and predicted values. One also notices that only surfaces A and M1 are far from the trend, which has not yet been explained at this level. This good general trend leads us to conclude that our model can capture some of the physics involved in the phenomenon of the generation of rolling resistance forces by the asperities of road surfaces.

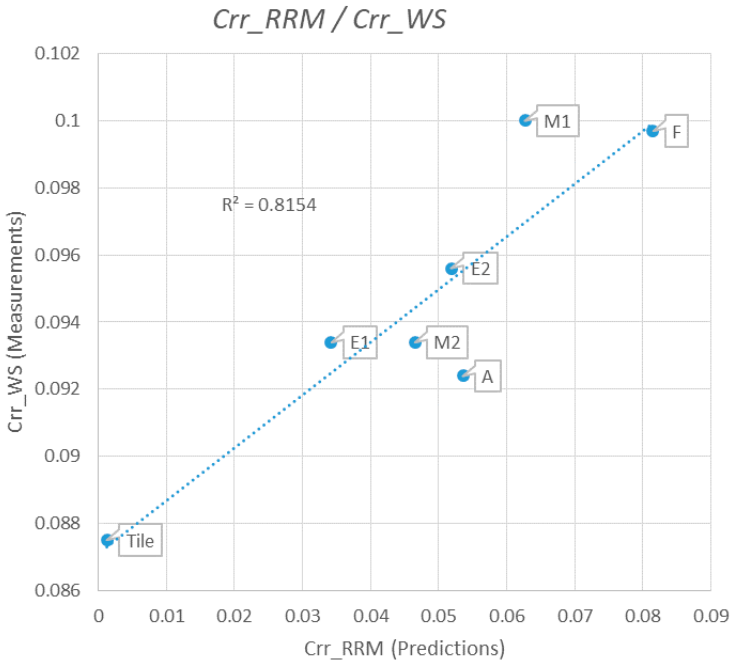


Figure 5. Correlation line between Crr_ RRM and Crr_WS.

Figure 6 shows the correlation line between the MPD of the surfaces and the Crr_RRM. One can also notice here the very good correlation, with an R^2 higher than 0.86, but once again the surfaces A and M1 are out of this trend. One can conclude that the contribution to the rolling resistance due to the pavement asperities increases with the macrotexture. This was confirmed by the direct comparison between Crr_WS and MPDs (Figure 7).

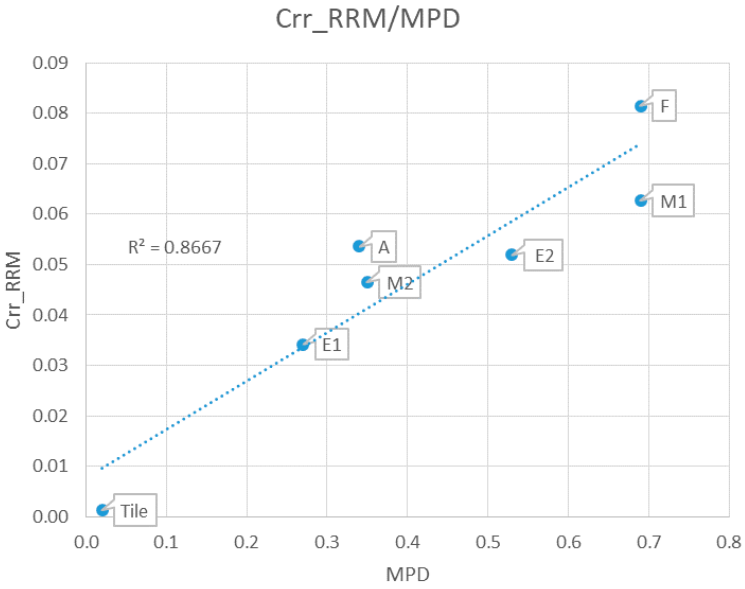


Figure 6. Correlation line between the MPD and Crr_RMM.

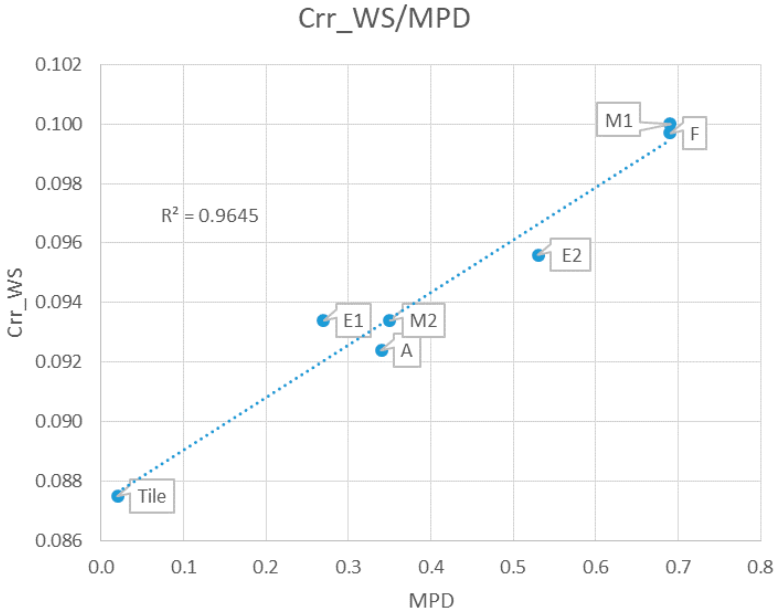


Figure 7. Comparison between Crr_WS and MPDs.

5. Discussion

Globally the texture contribution in rolling resistance increases with its macrotexture (Figure 6). This was expected intuitively. Indeed, the higher the obstacle to be overcome is, the greater the energy dissipated will be. Knowing that a higher macrotexture implies larger asperities, the increase in rolling resistance with increasing macrotexture can be explained. It can therefore be assumed that a smooth pavement (without adhesion) would minimize the rolling resistance, as the contribution of the texture would be eliminated. However, a smooth pavement would be catastrophic for vehicle traction in wet conditions. This led to us thinking about the optimization of this macrotexture to satisfy the antagonistic performances of these surfaces (thus minimizing the rolling resistance without adversely affecting the skid resistance).

Moreover, it should be noted that the random distribution and pointed shape of the asperities are an inconvenience for rolling resistance. Indeed, comparing the textures of surfaces F and M1 (Figure 4), the first one seems visually to have a much lower macrotexture (even if the calculation of the MPD gives the same value to the two surfaces), whereas these two surfaces display the same experimental Crr (Crr_WS) and even a higher Crr_RRM for F with the model (Figure 5). This can be explained by the positive texture of the latter, characterized by very prominent and randomly distributed asperities. This leads to the conclusion that beyond the macrotexture, the positive or negative distribution (F, A, and M1) of the texture should also be taken into account in predictions of the contribution of the surface on the rolling resistance.

We can also consider a simplification of the model. Indeed, this model, resulting from the simplification of the DFM model, only considers the tire rolling. It is, therefore, necessary to ask whether the damping component of the rubber is taken into account (thus considering the material of the tread as elastic and not viscoelastic). Indeed, knowing that each rubber element of the tread will keep contact with its opposite on the road from its entry to its exit of the contact and without any slip, it seems that we could do without the viscous part in the equations. This simplification would make the computational program much faster and less expensive in terms of data storage. Indeed, we would not need to store the displacements and other parameters of the previous time step.

It should also be noted that the temperature is not taken into account in the model. However, in real life, this parameter should be taken into account, because its rise tends to soften the rubber and thus the rolling resistance. We can also point out the two-dimensional aspect of the model, which also limits its accuracy. Indeed, the evolution of the latter in

three dimensions may allow its improvement, because it will take into account the real aspect in both directions of the texture, and the model will take into account the transverse interaction of the rubber elements.

6. Conclusions

This paper dealt with the modeling of rolling resistance on road pavements and included a discussion on the effect of macrotexture on the contribution of this rolling resistance. The proposed model is based on the simplification of the DFM, which is a tire/pavement adhesion model taking into account all the possible slip rates of a tire on the pavement ranging from 0 to 1. For its adaptation, all the parts related to the slip were removed to leave only the pure rolling as kinematic conditions. The model was tested on a set of surfaces differentiated by their macrotexture and validated by measuring the rolling resistance on these surfaces via an assembly from the WS machine in the laboratory. The results show that the texture contribution to the rolling resistance increased with the macrotexture, which would be due to larger stones that needed to be overcome. In addition, it should be noted that the random distribution and the pointed shape of the summits may be an inconvenience with respect to rolling resistance. It was also noted a possible simplification of the model by neglecting the damping part in the constitutive equations of the rubber was also noted.

Author Contributions: Data curation, E.R. and M.-T.D.; Formal analysis, E.R. and M.-T.D.; Investigation, M.K. and M.-T.D.; Methodology, M.K.; Writing—original draft, M.K.; Writing—review & editing, E.R. and M.-T.D. All authors have read and agreed to the published version of the manuscript.

Funding: This research received no external funding.

Institutional Review Board Statement: Not applicable.

Informed Consent Statement: Not applicable.

Data Availability Statement: Data supporting reported results can be requested to the authors by email, they would be happy to share them.

Conflicts of Interest: The authors declare no conflict of interest.

References

1. Chen, Y.; Ardila-Gomez, A.; Frame, G. *Achieving Energy Savings by Intelligent Transportation Systems Investments in the Context of Smart Cities*; World Bank: Washington, DC, USA, 2016. [CrossRef]
2. Huo, H.; He, K.; Wang, M.; Yao, Z. Vehicle technologies, fuel-economy policies, and fuel-consumption rates of Chinese vehicles. *Energy Policy* **2012**, *43*, 30–36. [CrossRef]
3. Global.yokohamatire.net. Rolling Resistance and Fuel Consumption | TIRE CARE & SAFETY | THE YOKOHAMA RUBBER CO., LTD. 2014. Available online: https://www.y-yokohama.com/global/product/tire/learn/care_safety/rolling_resistance/ (accessed on 2 May 2021).
4. Guillou, M.; Bradley, C. *Fuel Consumption Testing to Verify the Effect of Tire Rolling Resistance on Fuel Economy*; Technical Paper 2010-01-0763; SAE International: Warrendale, PA, USA, 2010. [CrossRef]
5. Aldhufairi, H.S.; Olatunbosun, O.A. Developments in tyre design for lower rolling resistance: A state of the art review. *Proc. Inst. Mech. Eng. Part D J. Automob. Eng.* **2017**, *232*, 1685–1882. [CrossRef]
6. Chupin, O.; Piau, J.M.; Chabot, A. Evaluation of the structure-induced rolling resistance (SRR) for pavements including viscoelastic material layers. *Mater. Struct.* **2013**, *46*, 683–696. [CrossRef]
7. Pettinari, M.; Lund-Jensen, B.B.; Schmidt, B. Low Rolling Resistance Pavements in Denmark. In Proceedings of the 6th Eurasphalt and Eurobitume Congress, Prague, Czech Republic, 1–3 June 2016. [CrossRef]
8. Sandberg, U.; Haider, M.; Conter, M.; Goubert, L.; Bergiers, A.; Glaeser, K.; Schwalbe, G.; Zöller, M.; Boujard, O.; Hammarström, U.; et al. *Rolling Resistance—Basic Information and State-of-the-Art on Measurement Methods*; SP 1. Measurement Methods Source Models; Swedish National Road and Transport Research Institute: Linköping, Sweden, 2011; p. 102.
9. Andersen, L.G.; Larsen, J.K.; Fraser, E.S.; Schmidt, B.; Dyre, J.C. Rolling resistance measurement and model development. *J. Transp. Eng.* **2015**, *141*, 04014075. [CrossRef]
10. Ejsmont, J.; Owczarzak, W. Engineering method of tire rolling resistance evaluation. *Measurement* **2019**, *145*, 144–149. [CrossRef]
11. Bergiers, A.; Goubert, L.; Anfosso-Lédée, F.; Dujardin, N. *Comparison of Rolling Resistance Measuring Equipment*. Technical Report for Pilot Study. 2011, p. 96. Available online: http://urn.kb.se/resolve?urn=urn:nbn:se:vti:diva-15697 (accessed on 2 May 2021).

12. Roveri, N.; Pepe, G.; Carcaterra, A. OPTYRE—A new technology for tire monitoring: Evidence of contact patch phenomena. *Mech. Syst. Signal Process.* **2016**, *66*, 793–810. [CrossRef]
13. Ejsmont, J.A.; Ronowski, G.; Świeczko-Żurek, B.; Sommer, S. Road texture influence on tyre rolling resistance. *Road Mater. Pavement Des.* **2017**, *18*, 181–198. [CrossRef]
14. Nielsen, L.; Sandberg, T. A new model for rolling resistance of pneumatic tires. *J. Passeng. Car Mech. Syst. J.* **2002**, *111*, 1572–1579.
15. Ai, J.; Chen, J.-F.; Rotter, J.M.; Ooi, J.Y. Assessment of rolling resistance models in discrete element simulations. *Powder Technol.* **2011**, *206*, 269–282. [CrossRef]
16. Ebbott, T.G.; Hohman, R.L.; Jeusette, J.-P.; Kerchman, V. Tire temperature and rolling resistance prediction with finite element analysis. *Tire Sci. Technol.* **1999**, *27*, 2–21. [CrossRef]
17. Clark, S. Geometric Effects on the Rolling Resistance of Pneumatic Tyres. In *Tire Rolling Losses and Fuel Economy*; Society of Automotive Engineers: Warrendale, PA, USA, 1977.
18. Sidharth, B.M.R. Tyre Modelling for Rolling Resistance. Master's Thesis, Chalmers University of Technology, Göteborg, Sweden, 2014. Available online: https://hdl.handle.net/20.500.12380/200040 (accessed on 2 May 2021).
19. Kane, M.; Edmondson, V. Tire/road friction prediction: Introduction a simplified numerical tool based on contact modelling. *Veh. Syst. Dyn.* **2020**, 1–20. [CrossRef]
20. Kane, M.; Do, M.-T.; Cerezo, V.; Rado, Z.; Khelifi, C. Contribution to pavement friction modelling: An introduction of the wetting effect. *Int. J. Pavement Eng.* **2019**, *20*, 965–976. [CrossRef]
21. Riahi, E.; Ropert, C.; Do, M.-T. Developing a laboratory test method for rolling resistance characterisation of road surface texture. *Surf. Topogr. Metrol. Prop.* **2020**, *8*, 024006. [CrossRef]